Assessing Low-GWP Refrigerants in Ground Source Heat Pump Systems: Long-Term Thermal Performance under Varied Geological Conditions and Cold Climate

Zilong ZHAO[1]*, Guoquan LV[2,3]*

[1] Thermo King Headquarters, Trane Technologies, Minneapolis, MN, USA.
zilong.zhao@tranetechnologies.com

[2] Department of Architecture, Zhejiang University, Hangzhou, China
[3] Center for Green Building and Low-Carbon City, International-Campus, Zhejiang University, Haining, China
guoquanlv@intl.zju.edu.cn

* Corresponding Author

ABSTRACT

The existing ground source heat pump (GSHP) systems are widely utilizing R410A as the primary refrigerant. As a replacement for R22, which was phased out due to its ozone-depleting potential, R410A can operate at a higher pressure and deliver improved energy efficiency in heat pump systems. However, the urgent objective of achieving carbon neutrality in the coming decades necessitates a continuous reduction in greenhouse gas emissions. This can be realized by incorporating more low-global warming potential (low-GWP) refrigerants into GSHP systems. Simultaneously, it is crucial to recognize that the subsurface environment may affect the thermal efficiency of the refrigeration system, which has not been examined in documented studies. In this study, a typical residential building operating under cold climate is first created and dynamically modeled in TRACE3D Plus. Furthermore, two most potentially applicable alternatives—R454B and R32 are explored as the working fluids in a GSHP model in TRNSYS. To evaluate the long-term impacts of different refrigerants on the subsurface overcooling and the degradation of GSHP efficiency, a lifespan operation of GSHP combining the building load profile is simulated. In the meantime, to assess the responsiveness of different refrigerants to environmental fluctuations, sets of heterogeneous geological units, comprised of varied ground thermal conductivities, layered thickness, and ground heat capacities, are integrated into the model as inputs. The varied thermal behaviors exhibited by refrigerants are carefully examined to analyze their influence on the heat pump operation. The results showed non-negligible differences when obtaining the annual coefficient of performance (COPs) and excessive ground cooling resulting from different combinations of refrigerants and diverse geological contexts. This study may provide insights for future optimization of GSHP systems.

1. INTRODUCTION

The ground source heat pump (GSHP) system utilizes a stable subsurface thermal environment and realizes effective heat transfer between the geological units and the working fluid in the ground heat exchanger (GHE). The seasonal conditioning demands from the building can then be fulfilled in avoid of drastic temperature difference between the ambient air source and the indoor environment, which typically leads to higher efficiency of the heat pump and thus lower the carbon footprints. As the urgently required carbon reduction plan undergoes, the implementation of renewable energy-based heat pump such as GSHP is highly desired. Over the last few years, plenty of studies involving GSHP have been focused on the optimization of design and operation strategies (Lee et al., 2023; Zhao et al., 2024a; Lu et al., 2023). Hybrid GHSP systems by combining solar assisted devices have proved that the overcooling issues in the subsurface can be effectively reduced, especially in the cold regions (Naili and Kooli, 2021; Chen et al., 2022; Zhao et al., 2022). Using boreholes as thermal storage and combining the geothermal storage with power grid is recognized as a viable approach to mitigate the fluctuations of energy sources in a district renewable energy system (Sadeghi, Jalali and Singh, 2024; Li et al., 2023). The primary goal of these studies is to

explore the energy-saving potential of GSHP and thus further decrease its carbon emissions, making it more environmentally friendly.

However, there has been a lack of concentration on the performance of the can be directly affected by multiple factors—the selection of refrigerants, the design of heat exchangers, the operation conditions of compressors, etc. As one of the most crucial factors, the refrigerant plays an important role during the operation of heat pump (You and Wang, 2023). The selection of refrigerants may affect the efficiency (COP) of a specified heat pump system and directly influences the emissions from the system (Lee et al., 2022; Kim et al., 2023). On the other hand, in recent studies, it has been widely recognized that the geological variables may impose a significant uncertainty to the optimal design and long-term economics of GSHP (Zhao et al., 2021; Zhao et al, 2022). The spatial distribution of ground thermal properties is a crucial factor when designing the shallow geothermal applications (Mao et al., 2023; Mao et al., 2024). By considering the impacts of groundwater flow on the convection around borehole area, thermal response tests have shown that the thermal resistance of the borehole can be significantly reduced (Tang et al., 2023; Magraner et al., 2021; Chae et al., 2020). And when the stochastic uncertainties of geological variables are integrated into the design process of GSHP, it has been found that the optimal length of borehole must be extended to ensure the system reliability (Zhao et al., 2024b). Therefore, it is crucial to coherently address both the selection of refrigerants and geological contexts when involving the long-term performance evaluation of GSHP system. This study thus develops a transient GSHP model in TRNSYS that is coupled to the refrigerant-based heat pump performance and varied ground thermal properties. The energy modeling to the building is first introduced in Section 2. The demonstration of refrigerants and geological properties is presented in Section 3, and the results and conclusions are included in Sections 4 and 5.

2. BUILDING ENERGY MODELING

To ensure the high fidelity of building energy demands, a complete one-year building energy modeling and simulation has been conducted in Trace3DPlus ("TRACE® 3D Plus", 2024). A 20-story residential building is developed and located in Minneapolis, MN, USA. The climate of Minneapolis is classified as 6A by ASHRAE ("Climatic Data", 2021), which has a minimum average temperature of -10° to -5°F (-23.3 °C ~ -20.6°C) and thus heating-dominated. Figure 1 presents the three-dimensional outer view of the building and the floor plan for each level, which consists of four separate apartment units. Under the recorded local meteorological conditions, the annual ambient temperature profile and the total heating and cooling electricity consumptions are presented by Figure 2. It can be found that though the ambient temperature has a clear variation between summer and winter, the overall heating activities outweigh the cooling in terms of the air conditioning demand. The average heating capacity provided by the HVAC system in January is approximately 220.7 KW and the average cooling capacity is around 193.8 KW. In the meantime, the heating season is set to the 1st to the 120th day combined with the period of the 245th day to 365th day. In contrast, the cooling season starts from 121st to 244th day of a year. In the simulation, the hourly profile of heating and cooling demand is utilized to ensure a higher fidelity from the user end side.

a) 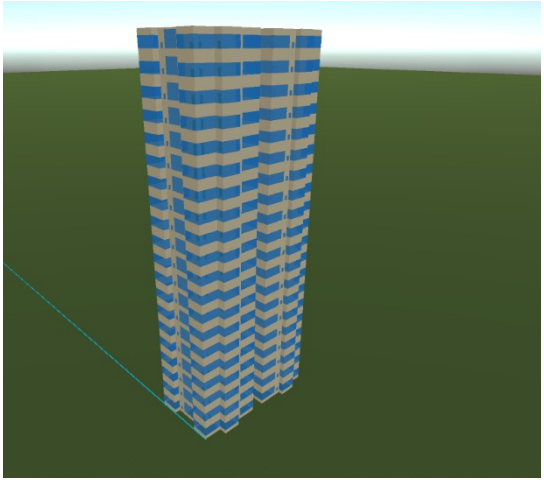 b) 

Figure 1: The three-dimensional view of the simulated building (a) and the floor plan (b) in Trace3DPlus.

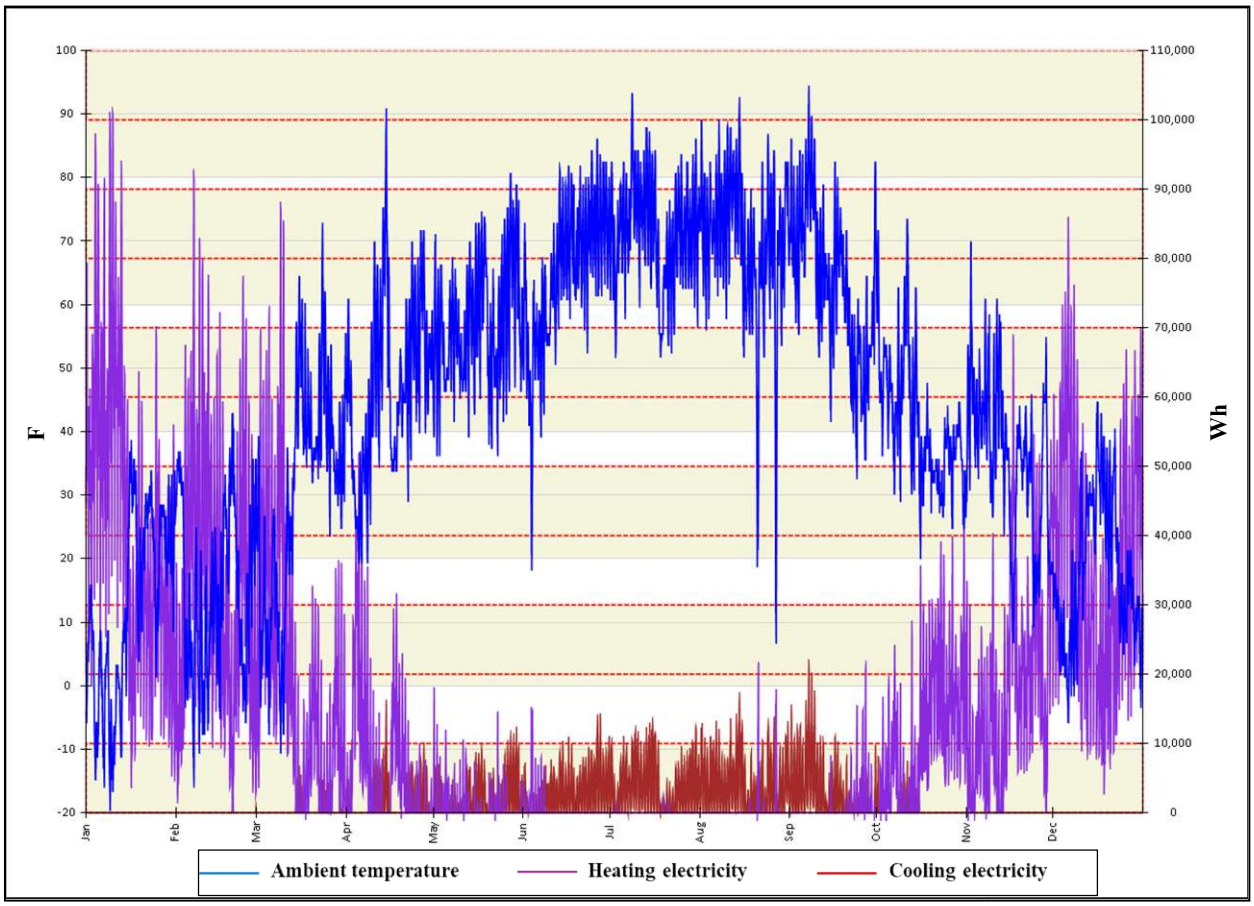

Figure 2: The dynamic profiles for the outdoor dry bulb temperature, total heating, and cooling electricity consumption over one year.

3. SELECTION OF REFRIGERANTS GEOLOGICAL CONFIGURATIONS

3.1 Alternative Refrigerants

The alternative refrigerants selected in this study include R32 and R454B due to their prospective features in applicability and environmental friendliness (Panato, Pico and Filho, 2022; Xia et al., 2023; Hsu, Chien and Chang, 2023). Their basic physical and thermal properties are compared and listed in Table 1. Note that all three types of refrigerants have an ozone depletion potential (ODP) of zero. And in contrast, R454B has the lowest global warming potential (GWP), as of 467. The boiling temperature of the baseline R410A is relatively lower than the two alternatives. To distinguish the difference among the heat pump system performances where different refrigerants are used, a simulated validation was conducted on a scaled small capacity heat pump unit using a one-dimensional heat pump model. As Table 2 demonstrates, the heat pump unit is run to achieve similar overall capacities while using the three selected refrigerants. Firstly, the boundary conditions are established at both the condenser and evaporator outlets, including the refrigerant temperature (23.9 ºC), subcooling temperature (5 ºC), and superheat temperature (10 ºC). Then, each refrigerant is integrated into the model, and a range of varied coolant entering temperatures at the evaporator and condenser are tested. The results of output exiting temperatures from the heat exchangers accompanied by the corresponding COPs are obtained. The correlation between the system outputs (COP, evaporator/condenser exiting temperatures) and inputs (refrigerants, evaporator/condenser entering temperatures) is explored by using linear regression in MATLAB and implemented into the TRNSYS model.

Table 1: Comparison of refrigerants' properties and characteristics among R410A, R32, and R454B.

Refrigerants	Molar mass (g/mol)	Boiling point at 1.0 bar (°C)	Critical temperature (°C)	Critical pressure (bar)	ODP	GWP
R410A	72.6	-48.5	72.8	49.0	0	2088
R32	52.0	-51.7	78.4	57.8	0	675
R454B	62.6	-50.1	77.0	52.7	0	467

Table 2: One set of refrigeration system configurations for simulating the performance of different refrigerants. Extreme conditions are used to generate more comprehensive performance characteristics of refrigerants.

	R410A	**R32**	**R454B**
Volumetric flow rate [cm^3/h]	100.9	73.9	94.3
Condenser Refrigerant Inlet			
Pressure [Psi]	260.1	262.5	247.2
Temperature [ºC]	73.3	90.6	82.0
Dew point temperature [ºC]	28.1	27.6	29.3
Condenser Refrigerant Outlet			
Specific enthalpy [kJ/kg]	237.8	243.4	240.1
Temperature [ºC]	23.9	23.9	23.9
Subcooling temperature [ºC]	5	5	5
Condenser capacity [kW]	6.22	7.02	7.26
Evaporator Refrigerant Inlet			
Pressure [Psi]	117.1	115.64	110.28
Temperature [ºC]	0.28	-0.61	-0.11
Dew point temperature [ºC]	0.36	-0.61	1.1
Evaporator Refrigerant Outlet			
Specific enthalpy [kJ/kg]	422.2	519.0	460.2
Temperature [ºC]	-8.0	-5.1	-7.3
Superheat temperature [ºC]	10	10	10
Evaporator capacity [kW]	5.52	6.21	5.66

3.2 Establishment of GHE Configurations

Serving as one of the key components in the study, Type 557 in TRNSYS is used to simulate the heat transfer process in GHE. The borehole configuration is presented in Table 3. To match the heating and cooling demand of the building, a 50-borehole field is designed with a constant depth of 100 m for each. The outer and inner dimensions of the ground loop pipe are used as default values, 0.0166 and 0.0137 m, respectively. To introduce geological heterogeneity, two additional sets of geological units are designed in this study that represent more intensive heat transfer ability in the subsurface. In the study of Zhao et al. (2023), an in-situ GSHP system was examined, and the heterogeneous geological environment is quantified using layered information. In another case study in Japan, Bina et al. (2020) evaluated the improvement of ground thermal conductivity in the region with the active groundwater flow. These case studies show significant differences in the heat transfer ability of the subsurface material that may occur due to the groundwater seepage and other complex geology. Therefore, the thermal conductivities of the layered geology presented in these two documented studies are simplified and incorporated into the TRNSYS GHE model, serving as two heterogeneous settings that can be compared to the baseline model. The details are listed in Table 4, as one can observe, the ground thermal conductivities in the two additional cases are 1.5

and 3 times of the original value used in the baseline. Other variables such as pipe dimensions and insulation performance can also be found in the table.

Table 3: Configurations of GHE applied in TRNSYS

Parameters	**Values**
Borehole depth	100
Number of boreholes	50
Borehole radius	0.075
Number of boreholes in series	5
Outer radius of pipe	0.0166
Inner radius of pipe	0.0137
Center-to-center distance	0.0508

Table 4: Comparison of different sets of geological thermal properties and layer thicknesses used in the simulation.

	Baseline	**Heterogeneity A**	**Heterogeneity B**	**Unit**
Total depth of borehole	100	100	100	m
Fill thermal conductivity	1.5	1.5	1.5	W/(mK)
Pipe thermal conductivity	0.5	0.5	0.5	W/(mK)
Insulation thickness	0.025	0.025	0.025	m
Insulation thermal conductivity	0.56	0.56	0.56	W/(mK)
Number of ground layers	1	3	3	N/A
Layer 1 thermal conductivity	1.5	2.0	3.79	W/(mK)
Layer 1 heat capacity	1	2.0	2.0	KJ/m^3K
Layer 1 thickness	100	22.4	30	m
Layer 2 thermal conductivity	-	2.3	5.65	W/(mK)
Layer 2 heat capacity	-	1.8	2.0	KJ/m^3K
Layer 2 thickness	-	16.3	30	m
Layer 3 thermal conductivity	-	2.8	4.53	W/(mK)
Layer 3 heat capacity	-	1.6	2.0	KJ/m^3K
Layer 3 thickness	-	61.3	40	m

3.3 General Settings in TRNSYS

Presented by Figure 3, the TRNSYS model is mainly comprised of three subsystems—the GHE module, the user end module, and the refrigerant-dependent heat pump module, whereas the user end module primarily collects the building energy demands over time and transfers the coolant outlet temperature and mass flow rates to the heat pump unit; the heat pump unit receives the physical information of two streams of coolants and calculate the output temperatures of them according to the correlations determined by the type of refrigerants. The transient ambient air temperature is also implemented in the GHE module for higher fidelity. The simulation time step is set to be one hour, and a ten-year period of operation is conducted. The time-dependent COPs, soil temperatures, etc. are received by the output data recorder and used for the subsequent data analysis.

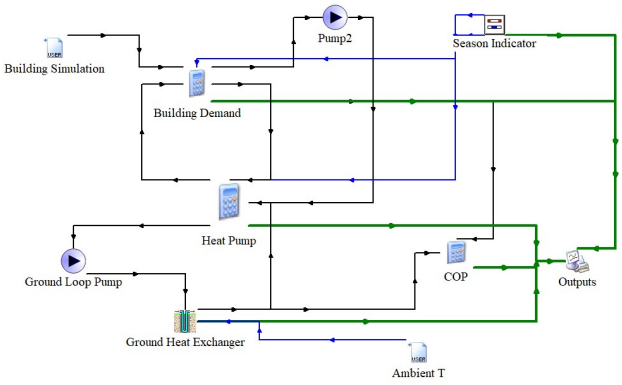

Figure 3: GSHP system configuration in TRNSYS.

4. RESULTS AND DISCUSSIONS

To evaluate the impacts of using different refrigerants, a ten-year simulation on a GSHP operation is accomplished. The variation of soil average temperature and the working fluid temperature at the outlet of the GHE are calculated and presented in Figure 4. As mentioned earlier, the simulation is conducted under a heating-dominated environment, and thus one should expect that the heat in the subsurface tends to be extracted that leads to a gradual temperature decrease over years. As one can observe, when using R454B, the annual decreases in both soil temperature and GHE outlet fluid temperature are mitigated. In contrast, when using R32, though it exhibits lower GWP, when it comes to long-term operation of GSHP in a cold region, the overcooling issue in the subsurface tends to be more severe. At the end of heating season at 10th simulation year, the subsurface temperature reaches the minimum. When using R32, the soil temperature drops to approximately -0.29 ºC, and the GHE outlet temperature reaches -1.87 ºC. R410A and R454B, however, deliver a minimum of 2.21 ºC and 4.36 ºC soil temperature. The COPs when using different refrigerants are also obtained and shown by Figure 5. In this comparison, however, R32 yields higher COP starting from the first year of operation, especially during the cooling seasons. The ten-year-average COP when using R32 is 3.37, higher than 3.07 when using R410A and 3.10 when using R454B. To be more specific, during the cooling season at the 10th simulation year, R32 yields COP around 3.34, while R410A and R454B yield 2.87 and 2.78 respectively.

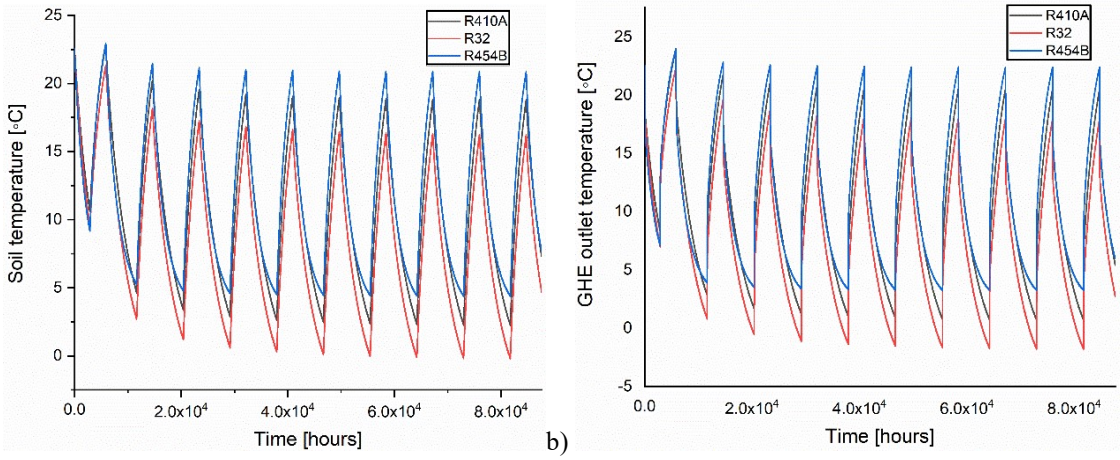

Figure 4: The variation of soil temperature (a) and GHE outlet working fluid temperature (b) over time.

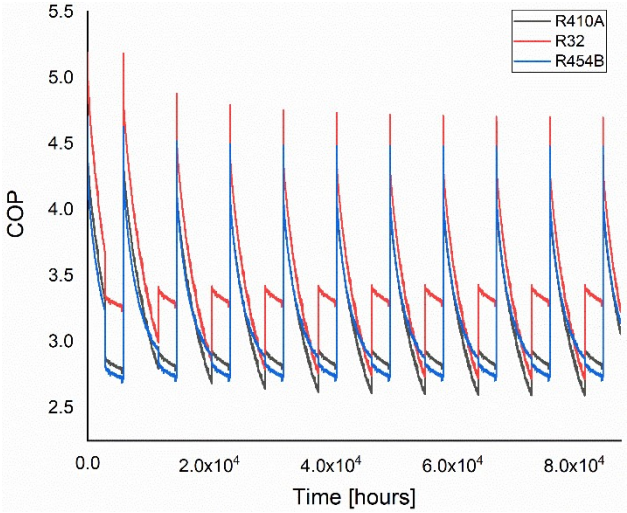

Figure 5: The COP evolution over time.

After exchanging heat with the fan coil at the user end, the coolant experiences a temperature drop in winter and a temperature rise in summer. This stream of coolant ultimately returns to the condenser, and its temperature depends on both the building energy demand at the specific time and the supply temperature of the coolant before entering the user end loop. Figure 6 shows its dynamic temperature profile when utilizing different refrigerants. And it can be found that R32 may increase the condenser outlet coolant temperature to maximum 33.5 ºC in heating season when compared to the other two selections. This may expectedly improve the efficiency of the heat pump and echoes the COP results demonstrated earlier. When using R410A and R454B in heating season, the entering temperature to the heat pump exhibits similar trends, while in cooling season, system using R410A shows a higher minimum temperature of 1.62 ºC, compared to 0.76 ºC when using R454B.

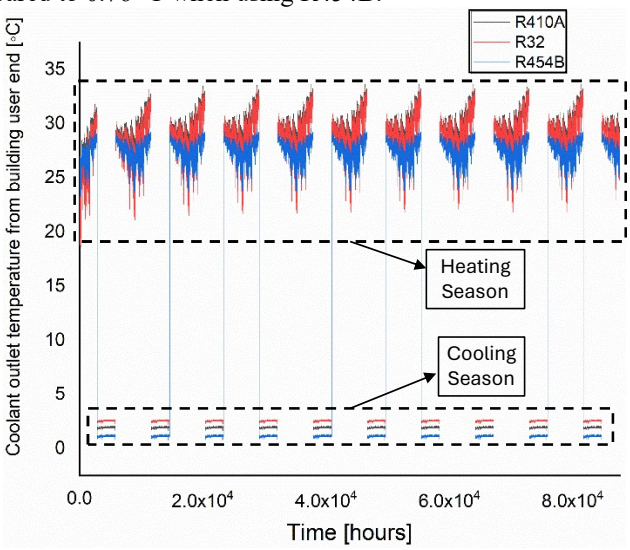

Figure 6: Outlet water temperature to the building (entering temperature to the heat pump) over time.

The impacts of heterogenous, high thermal conductive geology on the performance of refrigerant have been shown in Figure 7 using R410A as an example. As the results show, when elevating the magnitude of thermal conductivity, the COP is significantly improved during all seasons. The ten-year-average COP in the baseline, case A and case B are obtained as 3.07, 3.27, and 3.59, respectively. When concentrating on the last three months of the simulation, the heating season COPs are shown as 2.94, 3.10, and 3.39, respectively in the three cases. This is also accompanied by the mitigated overcooling in the ground, as the decrease in soil temperature over long-term operation is significantly reduced in cases A and B. The minimum soil temperature reached in case A is around 5.8 ºC and in case B 11.9 ºC. Compared to the baseline, the thermal declination in the subsurface is reduced by 17.7% and 47.6%, respectively.

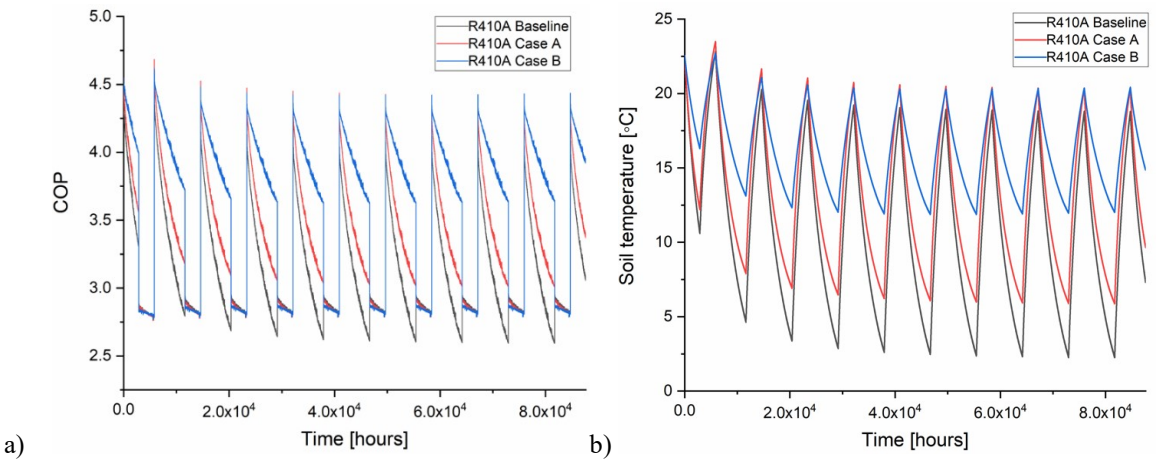

a) b)

Figure 7: Comparison of a) COP and b) soil temperature variation for refrigerant R410A when coupled with different sets of geological configurations.

To better show the coupled impacts of ground thermal conductivity and selection of refrigerants, the minimum soil temperature at each simulation year is collected for each of the nine cases and plotted over time to show the difference between the subsurface temperature drops. As Figure 8 illustrates, the thermal conductivity imposes a positive effect on reducing subsurface thermal anomaly when using any refrigerants. In the meantime, the alternative refrigerant R32 exhibits higher sensitivity to the change in ground thermal conductivity. As one can observe, R32 baseline yields the lowest soil temperature which reaches below 4.7 ºC at the end of the 10th year. However, in cases A and B, the soil temperature is elevated to be 7.3 ºC and 12.9 ºC, respectively. In contrast, R454B is least sensitive to the heat transfer performance of geology, though the minimum soil temperature at the end of 10th year is increased from 7.7 ºC to 12.4 ºC. Under extreme groundwater flow conditions, in case B, R410A yields highest soil temperature—least thermal imbalance in the subsurface, as the minimum soil temperature reaches 14.81 ºC, only 2.5 ºC lower compared to the end of the first simulation year.

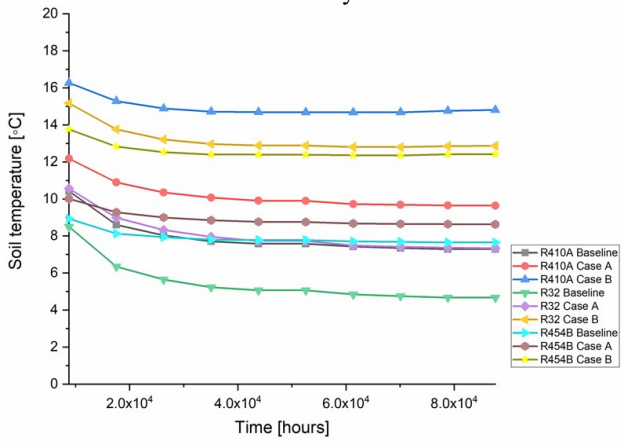

Figure 8: The lowest soil temperature at each simulation year over the long-term for different refrigerants combined with different ground thermal conductivities.

5. CONCLUSIONS

This study develops a GSHP model by incorporating the heterogeneous geology, characteristics of environmentally friendly refrigerants, dynamic building energy loads. A ten-year simulation is conducted and the key outputs, including variation in the system COP, evolution of soil temperature, and coolant temperature at the inlet of heat exchanger, are generated and analyzed. The primary conclusions can be obtained below.

- The impact of the selection of refrigerant on the system COP is non-negligible. When using R32, the average COP is found to be 3.37, which is 9.8% and 8.7% higher than that when using R410A and R454B.
- When using R454B, the thermal imbalance in the subsurface due to long-term GSHP operation can be better mitigated, as the minimum soil temperature at the end of simulation is 6.23 ºC and 2.15 ºC higher than R32 and R410A cases.
- When considering active groundwater flow and improved ground thermal conductivity, the drop of temperature in the subsurface can be reduced by up to 47.6% when using R410A.
- R32 exhibits highest sensitivity to the increase in ground thermal conductivity. At the end of the ten-year operation, the soil temperature increases by 8.2 ºC due to the higher ground thermal conductivity. While R454B shows highest stability with only 4.7 ºC increase in the same scenario.

NOMENCLATURE

COP	coefficient of performance	(–)
GSHP	ground source heat pump	(–)
GWP	global warming potentials	(–)

REFERENCES

ASHRAE (2021). Climatic Data for Building Design Standards. ISSN 1041-2336.

Bina, S. M., Fujii, H., Kosukegawa, H., & Farabi-Asl, H. (2020). Evaluation of ground source heat pump system's enhancement by extracting groundwater and making artificial groundwater velocity, Energy Convers. Manag. 223, 113298. https://doi.org/10.1016/j.enconman.2020.113298

Chae, H., Nagano, K., Sakata, Y., Katsura, T., Kondo, T. (2020). Estimation of fast groundwater flow velocity from thermal response test results, Energy Build. 206, 109571. https://doi.org/10.1016/j.enbuild.2019.109571

Chen, P., Liu, Y., Xu, Y., Ning, H., Qin, Y., Wang, Z. (2022). Performance of a solar ground source heat pump used for energy supply of a separated building, Geothermics. 105, 102524. https://doi.org/10.1016/j.geothermics.2022.102524

Hsu, C. H., Chien, L. H., Chang, J. C. (2023). Experimental study of falling film evaporation of refrigerants, R32, R1234yf, R410A, R452B and R454B on horizontal tubes, Int. J. Heat Mass Transf. 205, 123914. https://doi.org/10.1016/j.ijheatmasstransfer.2023.123914

Kim, J., Lee, M., Lee, D. C., Han, H., Y. Kim, Energy, economic, and environmental evaluation of a solar-assisted heat pump integrated with photovoltaic thermal modules using low-GWP refrigerants, Energy Convers. Manag. 293 (2023) 117512. https://doi.org/10.1016/j.enconman.2023.117512

Lee, M., Ham, S. H., Lee, S., Kim, J., Kim, Y. (2023). Multi-objective optimization of solar-assisted ground-source heat pumps for minimizing life-cycle cost and climate performance in heating-dominated regions, Energy. 270, 126868. https://doi.org/10.1016/j.energy.2023.126868

Lee, M., Kim, J., Shin, H. H., Cho, W., Kim, Y. (2022). CO2 emissions and energy performance analysis of ground-source and solar-assisted ground-source heat pumps using low-GWP refrigerants, Energy. 261, 125198. https://doi.org/10.1016/j.energy.2022.125198

Li, X., Yilmaz, S., Patel, M. K., Chambers, J. (2023). Techno-economic analysis of fifth-generation district heating and cooling combined with seasonal borehole thermal energy storage, Energy. 285, 129382. https://doi.org/10.1016/j.energy.2023.129382

Lu, S., Zhai, X., Wang, R., Wang, Z. (2023). System optimization and mode modification of the solar assisted ground source heat pump system for primary schools in northern rural areas of China, Sol. Energy. 263, 111879. https://doi.org/10.1016/j.solener.2023.111879

Magraner, T., Montero, A., Cazorla-Marín, A., Montagud-Montalvá, C., Martos, J. (2021). Thermal response test analysis for U-pipe vertical borehole heat exchangers under groundwater flow conditions, Renew. Energy. 165, 391-404. https://doi.org/10.1016/j.renene.2020.11.029

Mao, R., Zhao, Z., Tian, L., Fang, T., Wang, X. (2023). Generation of gridded temperature map of constant-temperature layer based on meteorological data for shallow geothermal applications, Geothermics. 113, 102770. https://doi.org/10.1016/j.geothermics.2023.102770

Mao, R., Zhao, Z., Tian, L., Wang, X., Maghirang, R. (2024). Mapping the Distribution of the Neutral Zone in Assist of Shallow Geothermal Applications in the United States. Proceedings, 49th Workshop on Geothermal Reservoir Engineering, Stanford University. SGP-TR-227.

Naili, N., Kooli, S. (2021). Solar-assisted ground source heat pump system operated in heating mode: A case study in Tunisia, Renew. Sustain. Energy Rev. 145, 111144. https://doi.org/10.1016/j.rser.2021.111144

Panato, V. H., Pico, M. D. F., Filho, E. P. B. (2022). Experimental evaluation of R32, R452B and R454B as alternative refrigerants for R410A in a refrigeration system, I. J. R. 135, 221-230. https://doi.org/10.1016/j.ijrefrig.2021.12.003

Sadeghi, H., Jalali, R., Singh, R. M. (2024). A review of borehole thermal energy storage and its integration into district heating systems, Renew. Sustain. Energy Rev. 192, 114236. https://doi.org/10.1016/j.rser.2023.114236

Tang, F., Jahangir, E., Luo, J., Nowamooz, H. (2023). Field hydrothermal identification with groundwater flow by conducting Distributed Thermal Response Test (DTRT) through Moving Line Source (MLS) theory, Appl. Therm. Eng. 230, 120740. https://doi.org/10.1016/j.applthermaleng.2023.120740

TRACE® 3D Plus. Accessed 2024. https://www.trane.com/commercial/north-america/us/en/products-systems/design-and-analysis-tools/trane-design-tools/trace-3d-plus.html

Xia, Y., Yu, J., Suulker, D., Wang, H. S. (2023). Flow boiling heat transfer of zeotropic mixture refrigerants R454B and R449A in a smooth horizontal tube, I. J. R. 150, 313-326. https://doi.org/10.1016/j.ijrefrig.2023.01.019

You, T., Wang, F. (2023). Green ground source heat pump using various low-global-warming-potential refrigerants: Thermal imbalance and long-term performance, Renew. Energy. 210, 159-173. https://doi.org/10.1016/j.renene.2023.04.058

Zhao, Z., Lin, Y., Stumpf, A., Wang, X. (2022). Assessing impacts of groundwater on geothermal heat exchangers: A review of methodology and modeling, 190, 121-147. https://doi.org/10.1016/j.renene.2022.03.089

Zhao, Z., Lv, G., Xu, Y., Lin, Y., Wang, P., Wang, X. (2024). Enhancing ground source heat pump system design optimization: A stochastic model incorporating transient geological factors and decision variables, 225, 120279. https://doi.org/10.1016/j.renene.2024.120279

Zhao, Z., Stumpf, A., Lin, Y., Wang, X. (2022). Impacts of prospective LEED building's energy loads on a borehole heat exchanger: A case study in Central Illinois, IGSHPA. http://dx.doi.org/10.22488/okstate.22.000030

Zhao, Z., Xu, Y., Lin, Y., Wang, X., Wang, P. (2021) Probabilistic modeling and reliability-based design optimization of a ground source heat pump system, Appl. Therm. Eng. 197, 117341. https://doi.org/10.1016/j.applthermaleng.2021.117341

Zhao, Z., Lv, G., Xu, Y., Lin, Y., Wang, P., Wang, X. (2024). A Stochastic Optimization Model for a Ground Source Heat Pump System with Uncertainty Quantifications on Transient Geologic Variables, Proceedings, 49th Workshop on Geothermal Reservoir Engineering, Stanford University. SGP-TR-227.

Zhao, Z., Lin, Y., Stumpf, A., Wang, X. (2023). Improving LEED-certified building loads on borehole heat exchangers by coupling subsurface variables, Appl. Therm. Eng. 224, 120119. https://doi.org/10.1016/j.applthermaleng.2023.120119